

CRC Project A-74/E-96

**Linking Tailpipe to Ambient:
Phase 1-3
Final Report**

May, 2014



COORDINATING RESEARCH COUNCIL, INC.

5755 NORTH POINT PARKWAY·SUITE 265·ALPHARETTA, GA 30022

The Coordinating Research Council, Inc. (CRC) is a non-profit corporation supported by the petroleum and automotive equipment industries and others. CRC operates through the committees made up of technical experts from industry and government who voluntarily participate. The four main areas of research within CRC are: air pollution (atmospheric and engineering studies); aviation fuels, lubricants, and equipment performance; heavy-duty vehicle fuels, lubricants, and equipment performance (e.g., diesel trucks); and light-duty vehicle fuels, lubricants, and equipment performance (e.g., passenger cars). CRC's function is to provide the mechanism for joint research conducted by the two industries and others that will help in determining the optimum combination of petroleum products and automotive equipment. CRC's work is limited to research that is mutually beneficial to the two industries involved, and all information is available to the public.

CRC makes no warranty expressed or implied on the application of information contained in this report. In formulating and approving reports, the appropriate committee of the Coordinating Research Council, Inc. has not investigated or considered patents which may apply to the subject matter. Prospective users of the report are responsible for protecting themselves against liability for infringement of patents.

Linking Tailpipe to Ambient

PHASE 1-3 FINAL REPORT

**ARB Project R1001
CRC PROJECT A-74/E-96
EPA STAR Project RD834554**

PERFORMING ORGANIZATION

Carnegie Mellon University
5000 Forbes Ave
Pittsburgh, PA 15213

PRINCIPAL INVESTIGATOR

Allen L. Robinson
Carnegie Mellon University
(412) 268 – 3657
e-mail: alr@andrew.cmu.edu

DATE

May 28, 2014

VERSION NUMBER: 1.2

Table of Contents

<i>Table of Contents</i>	<i>ii</i>
<i>List of Tables</i>	<i>iii</i>
<i>List of Figures</i>	<i>iv</i>
<i>List of Acronyms</i>	<i>vi</i>
<i>Acknowledgements</i>	<i>viii</i>
<i>Legal Notice</i>	<i>x</i>
<i>Executive Summary</i>	<i>1</i>
<i>List of Publications</i>	<i>24</i>

List of Tables

Table ES-1. Volatility distributions for gasoline and diesel vehicle POA collected on a quartz filter.

12

List of Figures

Figure ES-1. Experimental set-up used to characterize on-road vehicle emissions. Essentially the same set up was used for the off-road engines, except the engines were mounted on an engine dynamometer.	5
Figure ES-2. Compilation of gas-phase emissions data (2-stroke and 4-stroke SORE; cold-start UC tests of pre-LEV, LEV1, and LEV2 LDGVs; and non-DPF-equipped MDDV/HDDVs and DPF/DOC-equipped MDDV/HDDVs). a) CO; b) non-methane organic gases (NMOG); c) fraction of fuel carbon emitted as CO ₂ ; d) nitrogen oxides (NO _x = NO + NO ₂); and e) NO-to-NO _x mass ratio. One of the DPF-equipped diesel vehicles was outfitted with an SCR system. Results are compared to previous studies (symbols), where available.	6
Figure ES-3. Emission factors of a) gravimetric PM mass; b) organic carbon (OC); and c) elemental carbon (EC), Ratios of d) OC to EC and e) the sum of speciated PM components (1.2xOC, EC, and ions) to gravimetric PM mass. f) Mass fraction of speciated PM components. LDGV/MDDVs were testing using cold starts while HDDVs and SOREs are tested with hot starts. Symbols indicate data from previous studies.	8
Figure ES-4. Median emissions of speciated VOCs measured from all source categories. a) Absolute basis. b) Relative basis. Panel (b) also plots data for unburned fuel. Different protocols were used to speciate the gasoline and diesel vehicle exhaust (see text); further, LDGV/MDDVs were tested using vehicle cold start while HDDVs and SOREs followed hot-start procedures. Classes of compounds marked with an asterisk are considered to be SOA precursors. Footnotes: ¹ Diesel exhaust speciation protocol different than gasoline. ² Diesel fuel analysis extends to ~C ₃₀	10
Figure ES-5. Gas-phase and particle-phase evolution during a typical smog chamber experiment (SORE2S-1.1). Between -1.4 hr and -1.0 hr, the chamber was filled with dilute emissions from the backpack blower; between -1.0 hr and 0 hr, the primary PM was characterized; and after 0 hr, the UV lights were on and photo-oxidation generated SOA. Concentrations of NO, NO ₂ and O ₃ are shown in (a). Shown in (b) are the concentrations of three VOCs which are consumed by OH radicals during the photo-oxidation period. Shown in	

(c) are uncorrected and corrected (for wall-losses) organic PM concentrations using two different methods ($\omega=0$ and 1); the large increase is due to SOA production..... 16

Figure ES-6. (a) Measured wall-loss-corrected SOA concentration inside the smog chamber for LDGV experiments after 3 hours of photo-oxidation and (b) fractional contribution of background NMOG to smog chamber. The red braces in (a) indicate duplicate experiments. Hot-start and normal UC driving cycle experiments with two vehicles (LEV1-2 and LEV2-3) are denoted by the horizontal and diagonal black lines inside of the bars, respectively. The horizontal dashed red line in (a) indicates the minimum detection limit of the experiments. The dashed black lines in (b) indicate the median values of $\text{NMOG}_{\text{bkgd}}/\text{NMOG}_{\text{total}}$ for the three LEV classes. 20

Figure ES-7. Median EC and POA emissions and median SOA production from gasoline small off-road engines (SOREs), light-duty gasoline vehicles (LDGVs) and heavy-duty diesel vehicles (HDDVs). LDGV data were obtained during cold-start UC driving cycle experiments with a single CA summertime gasoline. There are three types of LDGV: pre-LEV vehicles were manufactured before 1995; LEV I vehicles were manufactured between 1995 and 2003; and LEV II vehicles were manufactured after 2003. HDDV data were obtained during UDDS driving cycle experiments with 3 different types of ULSD fuel. The HDDVs were either equipped with a diesel particulate filter (DPF) or no exhaust aftertreatment (no DPF). Error bars represent $\pm 1\sigma$. The absence of error bars for several of the SORE measurements is due to limited data for these sources..... 22

List of Acronyms

BC	Black carbon
C*	Effective saturation concentration
C ₆ -C ₁₂	Organic compounds with 6 to 12 carbon atoms
CAMx	Community Air Quality Model with Extensions
CARB	California Air Resources Board
CFR	Code of Federal Regulations
CMAQ	Community Multi-scale Air Quality Model
CMU	Carnegie Mellon University
CO	Carbon monoxide
CO ₂	Carbon dioxide
C _{OA}	Organic aerosol concentration
CRC	Coordinating Research Council
CTM	Chemical transport model
CVS	Constant volume sampler
DNPH	2,4-dinitrophenyl hydrazine
DOC	Diesel oxidation catalyst
DPF	Diesel particulate filter
EC	Elemental carbon
EPA	Environmental Protection Agency
FID	Flame ionization detector
GC	Gas chromatography
HDDV	Heavy-duty diesel vehicle
HONO	Nitrous acid
HSL	Haagen-Smit Laboratory
LDGV	Light-duty gasoline vehicle
LEV	Low emission vehicle
LEV1	Vehicle manufactured between 1994 and 2003 when the first California Air Resource Board Low Emission Vehicle standard was in place
LEV2	Vehicle manufactured after 2004 and present when the second California Air Resource Board Low Emission Vehicle standard was in place

MDDV	Medium-duty diesel vehicle
NMOG	Non-methane organic gases
NO	Nitric oxide
NO _x	Oxides of nitrogen
NO ₂	Nitrogen dioxide
OA	Organic aerosol
OH	Hydroxyl radical
OC	Organic carbon
POA	Primary organic aerosol
PM	Particulate matter
PM _{2.5}	Particulate matter with an aerodynamic diameter less than 2.5 micrometers
Pre-LEV	Vehicle manufactured before 1994 when the first California Air Resource Board Low Emission Vehicle standard was in place
RO ₂	Organoperoxy Radicals
SOA	Secondary organic aerosol
SORE	Small off-road engine
SVOC	Semivolatile organic compound
TD-GC-MS	Thermal desorption gas chromatography mass spectrometry
TRU	Transportation Refrigeration Unit
UC	Unified cycle (also known as 'LA-92')
UCM	Unresolved complex mixture
ULSD	Ultra-low sulfur diesel
UV	Ultraviolet
VOC	Volatile organic compound

Acknowledgements

This project would not have been possible without the dedication and hard work of a large team of researchers in the Center for Atmospheric Particle Studies at Carnegie Mellon University and the California Air Resources Board.

Carnegie Mellon University: Dr. Albert Presto (the Center for Atmospheric Particle Studies research manager) led the field campaigns and directed much of the research. Dr. Timothy Gordon was responsible for the smog chamber experiments and secondary organic aerosol analysis. Dr. Andrew May performed the gas-particle partitioning and sampling artifact analysis. Dr. Chris Hennigan has been instrumental in the development and application of the TD-GC-MS approach. Dr. Eric Lipsky (on the faculty at Penn State Greater Allegheny) was instrumental in helping to design and deploy the sampling system. Ngoc Nguyen helped with sample collection and TD-GC-MS analysis. Mrunmayi Karve performed the OC/EC analysis of the CMU filter samples. Dr. Shantanu Jathar worked on the secondary organic aerosol modeling. Prof. Peter Adams and Prof. Neil Donahue provided valuable guidance on data analysis and modeling.

The authors would like to acknowledge the contributions of many people at the California Air Resources Board, especially the hard work and dedication of the personnel at the Haagen-Smit and Heavy-Duty Vehicle Laboratories. Key contributors included Hector Maldonado, Sulekha Chattopadhyay, Paul Rieger, Richard Ling, Christine Maddox, Oliver Chang, Yanbo Pang, Shiou-Mei Huang, Mark Fuentes, Thu Vo, Mang Zhang, Jeff Long, Eileen McCauley, Todd Sax, Pablo Cicero, John Massetti, Shiyen Chen, Tin Truong, Thomas Ladzinski, Christian Hall, Subhasis Biswas, Kwangsam Na, Sahay Keshav, and William Robertson.

The authors would like to acknowledge the contributions of Dr. Matti Maricq of Ford, Dr. Timothy Wallington of Ford, Rory MacArthur of Chevron and the Coordinating Research Council Real World Group and Atmospheric Impacts Committee. Finally we thank Sherri Hunt at EPA.

Financial support for the project was provided by the following organizations: California Air Resources Board supported vehicle procurement, testing, and emissions characterization; the Environmental Protection Agency through the National Center for Environmental Research

(NCER) under a STAR Research Assistance Agreement No. RD834554 supported primary emissions measurements; and the Coordinating Research Council (Projects A-74/E-96) supported the smog chamber experiments.

Legal Notice

This report was prepared by Carnegie Mellon University (CMU) as an account of work sponsored by the Coordinating Research Council (CRC). Neither the CRC, members of the CRC, CMU nor any person acting on their behalf: (1) makes any warranty, express or implied, with respect to the use of any information, apparatus, method, or process disclosed in this report, or (2) assumes any liabilities with respect to use of, inability of use, or damages resulting from the use or inability to use, any information, apparatus, method or process disclosed in this report.

The report has not been formally reviewed by the EPA. The views expressed in this document are solely those of the authors, and the EPA does not endorse any products or commercial services mentioned in this publication.

Executive Summary

This project was motivated by the continuing need to improve ambient air quality. As of December 2012, more than 74 million Americans live in areas that violate the National Ambient Air Quality Standard for fine particulate matter (or $PM_{2.5}$). Organic aerosol often contributes between 30 and 60% of ambient fine particulate matter. However, the sources of ambient organic aerosols are not well understood and state-of-the-art chemical transport models often underpredict the measured organic aerosol concentrations by a factor of 2 or more. Better understanding of the sources of organic aerosols may be needed for the development of effective control strategies.

Motor vehicles are a source of primary organic aerosol (POA) and some secondary organic aerosol (SOA) precursors in urban areas. POA is organic aerosol that is directly emitted from a source; SOA is organic aerosol produced in the atmosphere from low-volatility reaction products of gaseous precursors. Although emissions from motor vehicles have been dramatically reduced since the early 1970s and fine particle levels in most urban areas are falling, mobile sources (on- and off-road) still contribute significantly to the national volatile organic compound, carbon monoxide, oxide of nitrogen, and fine particulate matter emissions. The fractional contribution of motor vehicles is often higher than other sources in urban areas. Therefore, vehicle emissions must be accurately represented in emission inventories and chemical transport models (CTMs) used to simulate atmospheric particulate matter (PM) concentrations.

When motor vehicle emissions leave the exhaust system, they are rapidly transformed in the atmosphere. Dilution and cooling of the emissions alters the gas-particle partitioning of the particulate emissions. Exposure to sunlight, other pollutants, and atmospheric oxidants such as ozone and the hydroxyl radical causes the emissions to evolve chemically. Some of the products of these reactions form secondary PM. These processes can dramatically affect the contribution of motor vehicle emissions to ambient particulate matter. Therefore, to quantify the contribution of motor vehicles to ambient PM levels, one must understand both direct particle emissions and PM formed in the atmosphere.

This report describes results from a three-phase test program that characterized the emissions from on-road gasoline vehicles, on-road diesel vehicles, and small off-road engines. The overarching goal of the project was to investigate the atmospheric transformations of mobile source emissions to better quantify their contribution to ambient PM levels – in other words to link tailpipe to ambient. This was done by characterizing the tailpipe emissions from in-use sources and by investigating the atmospheric evolution of the emissions using dilution tunnels and smog chambers. Specific objectives of the test program were to:

- measure emissions data for use in inventories and chemical transport models;
- characterize the gas-particle partitioning of primary organic aerosol emissions; and
- measure the secondary organic aerosol (SOA) production from photo-oxidation of dilute exhaust.

The new data are also being used to test the volatility basis set approach, a recently proposed computationally efficient treatment of gas-particle partitioning and aging of organic emissions from combustion systems. This conceptual model was developed based on “proof-of-concept” laboratory experiments conducted with emissions from a small diesel generator and wood-burning. This project investigates if the concept can be scaled from the laboratory to the real world by testing a sufficient population of in-use vehicles to capture the variability in real emissions and to subject these emissions to realistic atmospheric processing.

Vehicle Fleet and Test Methods: The Phase 1 experiments were conducted with 45 light-duty gasoline and two medium-duty diesel vehicles over a five-week period in May and June of 2010 at the California Air Resources Board Haagen-Smit Laboratory in El Monte, California. The Phase 2 experiments characterized the emissions from three heavy-duty diesel tractors over a six-week period in June and July of 2011 at the California Air Resources Board Heavy-Duty Vehicle Emissions Laboratory in Los Angeles, California. The Phase 3 experiments characterized the emissions from 21 gasoline-powered on-road vehicles and 7 off-road engines over a six-week period in January and February of 2012 at the Haagen-Smit Laboratory.

In total the test program tested the emissions of 66 unique on-road light-duty gasoline vehicles (LDGV) that were recruited from the in-use California fleet, including vehicles from southern California residents, rental car companies, and the California Air Resource Board

vehicle pool. The LDGV fleet was not designed to represent the distribution of vehicles in the current, in-use California fleet; instead the test vehicles were selected to span a wide range of model years (1987 to 2012), vehicle types, and emission control technologies. For discussion, the vehicles are grouped based on model year: “pre-LEV” are vehicles manufactured prior to 1995; “LEV1” vehicles are manufactured between 1995 and 2003; and “LEV2” vehicles are manufactured 2004 or later. In this work, the LEV designation simply refers to a range of model years; it does not refer to the emissions certification standard. The test fleet consisted of 15 pre-LEV vehicles, 26 LEV1 vehicles, and 25 LEV2 vehicles. Each gasoline vehicle was tested using a chassis dynamometer, the cold-start unified cycle, and commercial California summertime fuel. A subset of the vehicles was also tested using the hot-start unified, arterial, and freeway cycles.

In total the project tested five diesel vehicles, which were specifically chosen to span a range of emission aftertreatment technologies. Three of the diesel vehicles were heavy-duty tractors owned by the California Air Resource Board; each was powered with a typical six cylinder, in-line, direct injection, turbocharged, heavy-duty diesel engine. The three tractors were equipped with different types of emissions control technology: one had no exhaust aftertreatment, a second had a catalyzed diesel particulate filter (DPF), and the third had a catalyzed DPF and a selective catalytic reduction (SCR) unit. Each tractor was tested using a chassis dynamometer, the Urban Dynamometer Driving Schedule and other driving cycles. The final two vehicles were full-sized pickup trucks with gross vehicle weight ratings between 8,500 and 9,500 lbs and were classified as medium duty diesel vehicles (MDDV). One had a turbocharged V8 engine equipped with a diesel oxidation catalyst (DOC), and the other had a turbocharged inline 6 cylinder engine with no aftertreatment. The two MDDVs were tested using the cold-start unified cycle.

The project tested seven off-road engines: six gasoline-powered small off-road engines (SORE) used in a variety of applications (backpack leaf blower, soil tiller, string lawn trimmer and lawnmower) and one larger diesel engine from a transportation refrigeration unit (TRU). The SOREs included both 2- and 4-stroke engines manufactured between 2002 and 2006. All of the engines met the relevant certification standard. None of the off-road engines was equipped with a catalyst or other aftertreatment device to reduce emissions. The engines were not chosen with the specific goal of representing the diverse fleet of in-use SOREs and TRU engines, but to

provide an initial screening from a broad range of technologies. The engines were operated on an engine dynamometer following California Air Resources Board procedures for engine certification which are based on SAE J1088. The test cycles depend on engine size and application; briefly, each test cycle consists of two to six separate phases or modes during which the engine is operated at a specified speed and load. The emissions measured during each mode were then weighted based on expected product usage.

All of the vehicles/engines were tested using commercial fuels. The majority of the light-duty gasoline vehicles and all of the SOREs were tested using the same California summertime fuel; the remainder of the LDGVs were tested as-received, using the fuel that was in the tank when the vehicle was recruited. The heavy-duty diesel vehicles (HDDVs) were tested using three different ultra-low sulfur diesel (ULSD) fuels: low aromatic (9% aromatic content), mid-aromatic (12% aromatic content), and high aromatic (28% aromatic content). The mid-aromatic was commercial California ULSD; it was used as the base fuel for the experiments. Both of the MDDVs were tested with a commercial ULSD purchased from a local service station, which was expected to be comparable, but not identical, to the mid-aromatic ULSD used in the HDDVs. Fuel samples were collected from most vehicles and analyzed to determine average composition and properties.

Primary Emissions: Both standard and speciated emissions of gaseous and particulate pollutants were measured during each test. A schematic of the experimental set up is provided as Figure ES-1. Tailpipe emissions were sampled using constant volume sampling (CVS) systems (Horiba-7200 SLE), nominally following the procedures outlined in Code of Federal Regulations Part 86. Measured gaseous emissions included carbon monoxide (CO), carbon dioxide (CO₂), methane (CH₄), nitric oxide (NO), oxides of nitrogen (NO_x), and non-methane organic gases (NMOG). Filter samples were collected from the CVS to determine emissions of gravimetric PM mass, organic and elemental carbon, and major ions. Finally, quartz filter and Tenax™ TA sorbent samples were collected to characterize low-volatility organic emissions. Speciation was performed on the organic emissions, including quantification of carbonyls and C₂ to C₃₀ hydrocarbons. Background and blank measurements were collected to characterize potential sources of contamination.

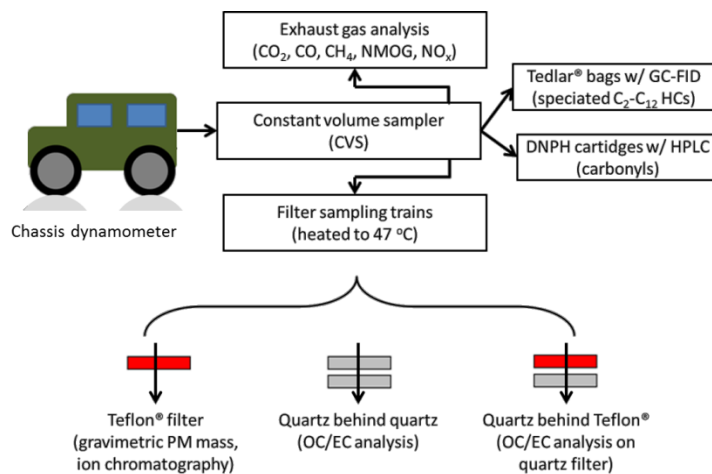


Figure ES-1. Experimental set-up used to characterize on-road vehicle emissions. Essentially the same set up was used for the off-road engines, except the engines were mounted on an engine dynamometer.

Figure ES-2 compiles gas-phase emissions data measured in the CVS, including CO, NMOG, fraction of fuel carbon emitted as CO₂, NO_x, and NO/NO_x fraction. The data are presented as box-and-whisker plots to illustrate the range of emissions for seven different source classes: pre-LEV, LEV1, LEV2, non-DPF-equipped diesel vehicles, DPF-equipped HDDVs, two-stroke gasoline SORE, and four-stroke gasoline SORE. Although there was variability within each source category, there are a number of clear trends in the overall dataset that are consistent with previous studies. Two-stroke gasoline SOREs had the highest CO and NMOG emissions of any sources tested in this study -- 10-100 times greater than the on-road LDGVs. The DPF-equipped diesels had the lowest NMOG and CO emissions. Four-stroke SOREs and non-SCR-equipped diesel vehicles had the highest NO_x emissions and LEV2 LDGVs had the lowest. Emissions from newer LDGVs were, on average, much lower than older LDGVs. For example, the NMOG emissions from median LEV1 LDGV were about a factor of three lower than the median pre-LEV LDGV; there was another reduction (factor of three) in NMOG emissions from the median LEV1 LDGV to the median LEV2 LDGV. The reduction in NO_x emissions from newer LDGVs was even more dramatic, with the median emissions from LEV2 LDGV being about a factor of 25 lower than the median pre-LEV LDGV.

As expected, the HDDVs equipped with exhaust aftertreatment had dramatically lower emissions than diesels without aftertreatment. The catalyzed DPF and DOC reduced emissions

of CO and NMOG by an order of magnitude or more compared to non-DPF-equipped vehicles. NO_x emissions from the SCR-equipped vehicle were 80% lower than from the non-aftertreatment-equipped vehicles.

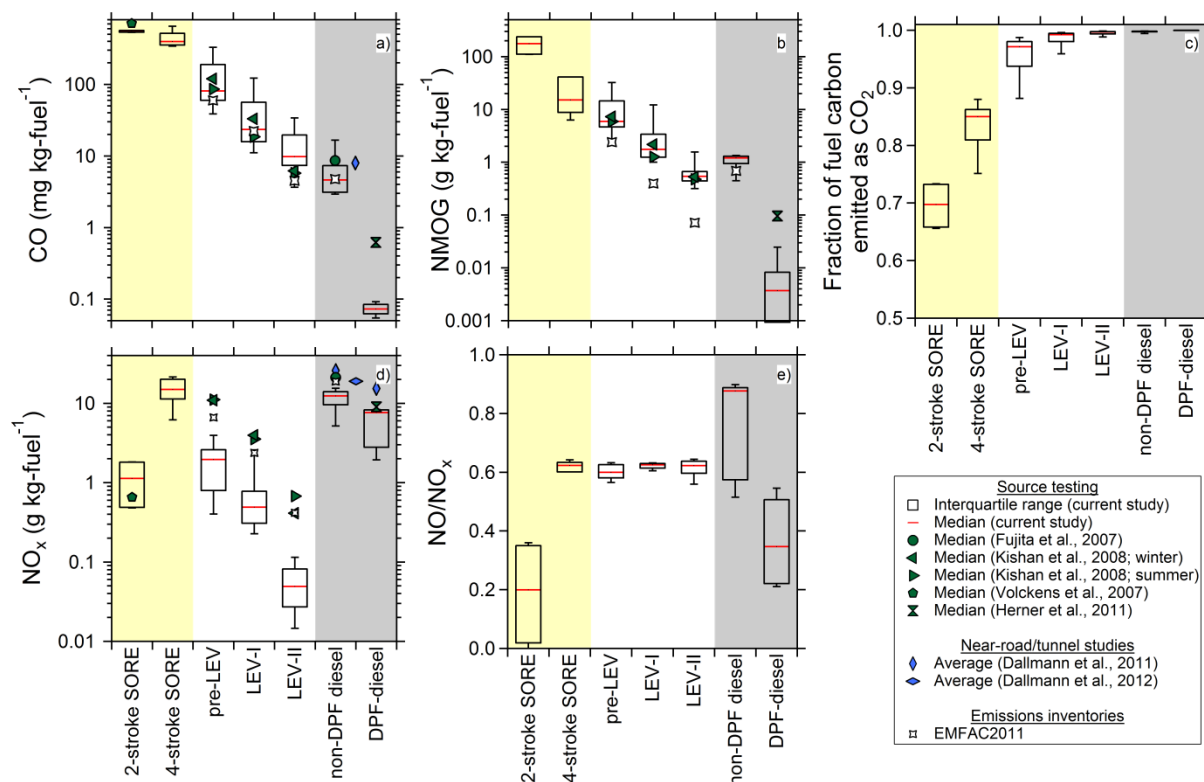


Figure ES-2. Compilation of gas-phase emissions data (2-stroke and 4-stroke SORE; cold-start UC tests of pre-LEV, LEV1, and LEV2 LDGVs; and non-DPF-equipped MDDV/HDDVs and DPF/DOC-equipped MDDV/HDDVs). **a)** CO; **b)** non-methane organic gases (NMOG); **c)** fraction of fuel carbon emitted as CO_2 ; **d)** nitrogen oxides ($\text{NO}_x = \text{NO} + \text{NO}_2$); and **e)** NO-to- NO_x mass ratio. One of the DPF-equipped diesel vehicles was outfitted with an SCR system. Results are compared to previous studies (symbols), where available.

Figure ES-3 summarizes the particulate matter (PM) emissions data measured using filters collected from the CVS, including gravimetric PM mass, organic carbon (OC), elemental carbon (EC), the ratio of OC to EC, the mass balance of the sum of speciated PM components to gravimetric mass, and the mass fraction of individual components present in the PM (OC, EC and targeted ions). Two-stroke gasoline SOREs had the highest PM emissions, followed by non-DPF-equipped diesels. Unlike the regulated gases (Figure ES-2), there was not a clear reduction in PM emissions with each successive class of LDGVs. PM mass emissions were reduced by

about a factor of three from pre-LEV to LEV1 LDGVs, but the LEV1 and LEV2 LDGVs had similar emissions of PM (although there was greater variability in the LEV1 PM emissions). This likely reflects the fact that LEV1 vehicles met the LEV2 PM standard, so there was no regulatory pressure to further reduce PM emissions as there was for other pollutants (e.g., NO_x or CO). There was a steep decreasing trend in OC emissions, which were reduced by a factor of ~20 from pre-LEV to LEV2 vehicles, roughly mirroring the reduction in NMOG emissions (Figure ES-2b). EC emissions (Figure ES-3c) were roughly constant across the three LDGV classes, but varied by nearly a factor of 10 within each class.

The diesel PM emissions data in Figure ES-3 followed the same basic trends as the criteria gases in Figure ES-2. The DPF-equipped diesel vehicles had gravimetric PM mass emissions that were over two orders of magnitude lower than the diesel vehicles with no DPF. The majority of this reduction was EC. There was also a reduction in OC emissions; however, the majority of the measured OC for the DPF-equipped vehicles during hot-start cycles was likely sampling artifact – adsorbed organic vapors collected on the quartz filter.

As expected, carbonaceous material contributed the majority of the primary PM mass. The ratio of speciated-to-gravimetric PM mass was close to unity for LDGVs, indicating good mass closure for the filter-based measurements. However, for the non-DPF-equipped diesels, the sum of the speciated components only accounted for about 50% of the gravimetric PM mass. Similar mass balance discrepancies have been reported previously for diesel PM. The cause of this discrepancy is not known. For the 4-stroke SORE and DPF-equipped diesel the sum of the speciated components was greater than the gravimetric PM mass. This discrepancy was thought to be due to positive sampling artifacts that commonly occur with quartz filters.

An important objective of this project was to quantify the secondary organic aerosol (SOA) formation. To better understand the SOA precursor emissions, comprehensive speciation was performed on the volatile organic compound emissions. Over 250 individual organic compounds were identified in the LDGV/MDDV exhaust, and over 100 organic compounds were identified in the HDDV exhaust. Figure ES-4 summarizes speciation data for tailpipe emissions and unburned fuels. The data are categorized into the following classes: CH₄, ethanol, light alkanes (C₂-C₆ straight/branched), mid-range alkanes (C₇-C₁₂ straight/branched), olefins/naphthenes,

cyclic olefins, polycyclic naphthenes, single-ring aromatics, polycyclic aromatics, non-aromatic carbonyls, aromatic carbonyls, and unspciated organics. Unspciated organics are defined as the difference between the total NMOG and the sum of the speciated compounds. These unidentified compounds are likely indistinguishable isomers that cannot be separated in the GC column (especially for HDDV exhaust) or are lower-volatility organic compounds that do not elute in the GC column yet are quantified by the NMOG flame ionization detector.

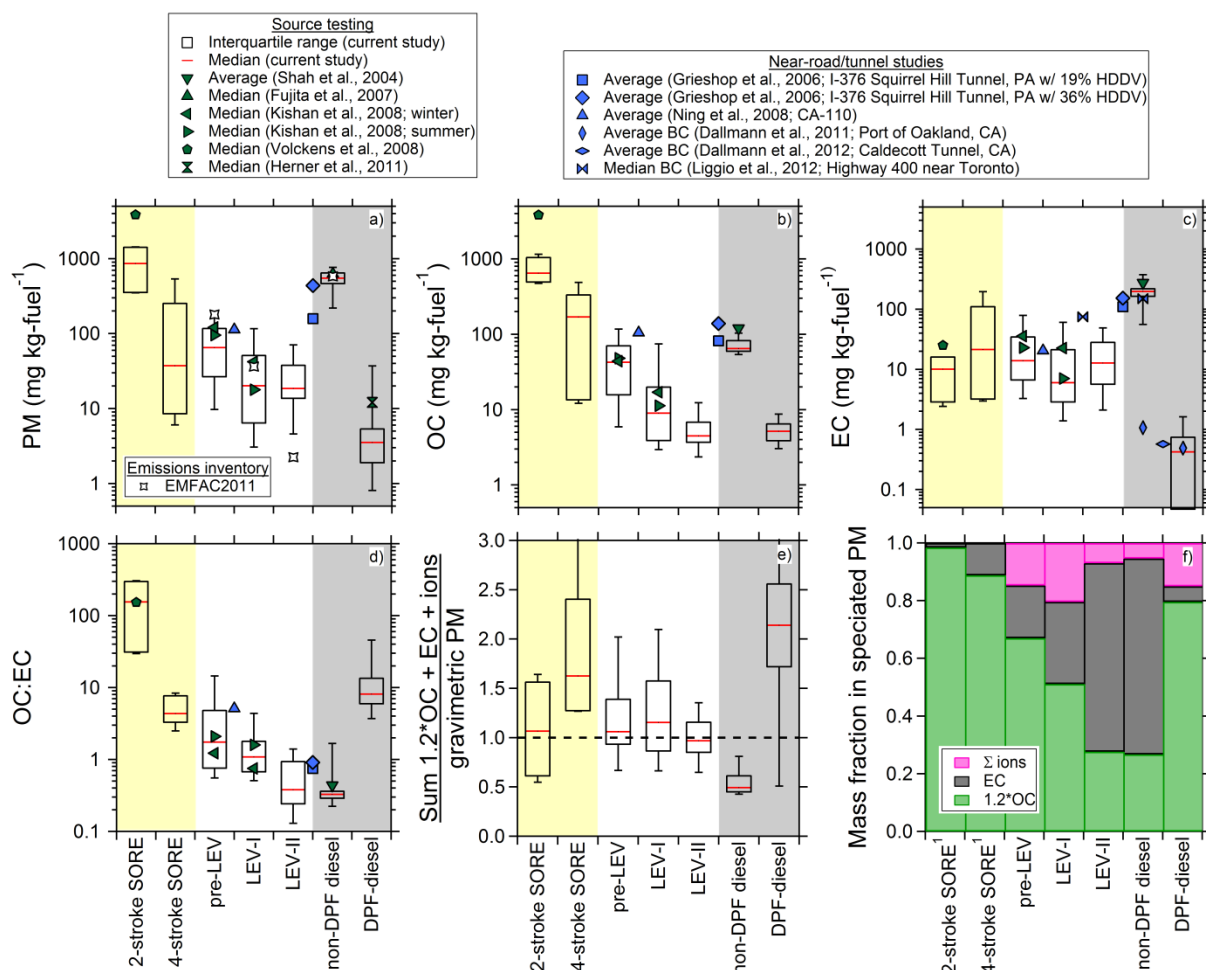


Figure ES-3. Emission factors of **a)** gravimetric PM mass; **b)** organic carbon (OC); and **c)** elemental carbon (EC), Ratios of **d)** OC to EC and **e)** the sum of speciated PM components (1.2xOC, EC, and ions) to gravimetric PM mass. **f)** Mass fraction of speciated PM components. LDGV/MDDVs were testing using cold starts while HDDVs and SOREs are tested with hot starts. Symbols indicate data from previous studies.

The NMOG composition from all three LDGV categories (pre-LEV, LEV1, and LEV2) was relatively similar, with ~15% single-ring aromatic, ~10% olefins/naphthenes, and ~40% normal/branched alkanes. About 25% of the NMOG emissions were not speciated, which is comparable to previous studies. These unspciated emissions are thought to be a complex mixture of lower molecular weight branched and cyclic alkanes. Both the two-stroke and four-stroke gasoline SORE exhaust composition share some similarities with LDGVs; the four-stroke gasoline SORE exhaust had a large amount of unidentified organics (~70%). Diesel exhaust has a somewhat different NMOG composition than the LDGV exhaust, which can be attributed to differences in fuels and combustion processes (compression versus spark ignition). For example, non-aromatic carbonyls (e.g., formaldehyde, acetaldehyde, acrolein) contributed ~15% of the identified NMOG mass from the non-DPF/non-DOC-equipped diesel vehicles, which is much higher than for the gasoline sources. There was also a larger fraction of unidentifiable compounds in the diesel exhaust (~70%) compared to the gasoline exhaust. This is not surprising since a large fraction (~60%) of the diesel fuel had a carbon number greater than C₁₂, which was the upper limit for the VOC speciation analysis.

The primary emissions data provide insight into the relative importance of primary PM emissions versus SOA formation. Aromatics and larger hydrocarbons (C₉ and larger) are known SOA precursors. The ratio of the emissions of speciated SOA precursors to primary organic aerosol provides a simple measure of the potential importance of SOA formation. For all pre-LEV and LEV1 LDGV, there were about 50 times more speciated SOA precursor emissions than primary organic aerosol emissions. For LEV-2 vehicles this ratio was about 30. This ratio depends on drive cycle – lower ratios were measured during hot-start UC LDGV compared to cold-start tests. This ratio was much greater for cold-start LDGVs (~20-90) than hot-start diesel vehicles (~2-4). Yields for aromatics and large alkanes are around 10% for typical atmospheric conditions. Therefore, the emissions data themselves indicate that the SOA formed from cold-start LDGV emissions will likely exceed the POA. For hot-start diesel emissions, the SOA and POA levels will likely be comparable. The hypotheses were verified by the smog chamber experiments.

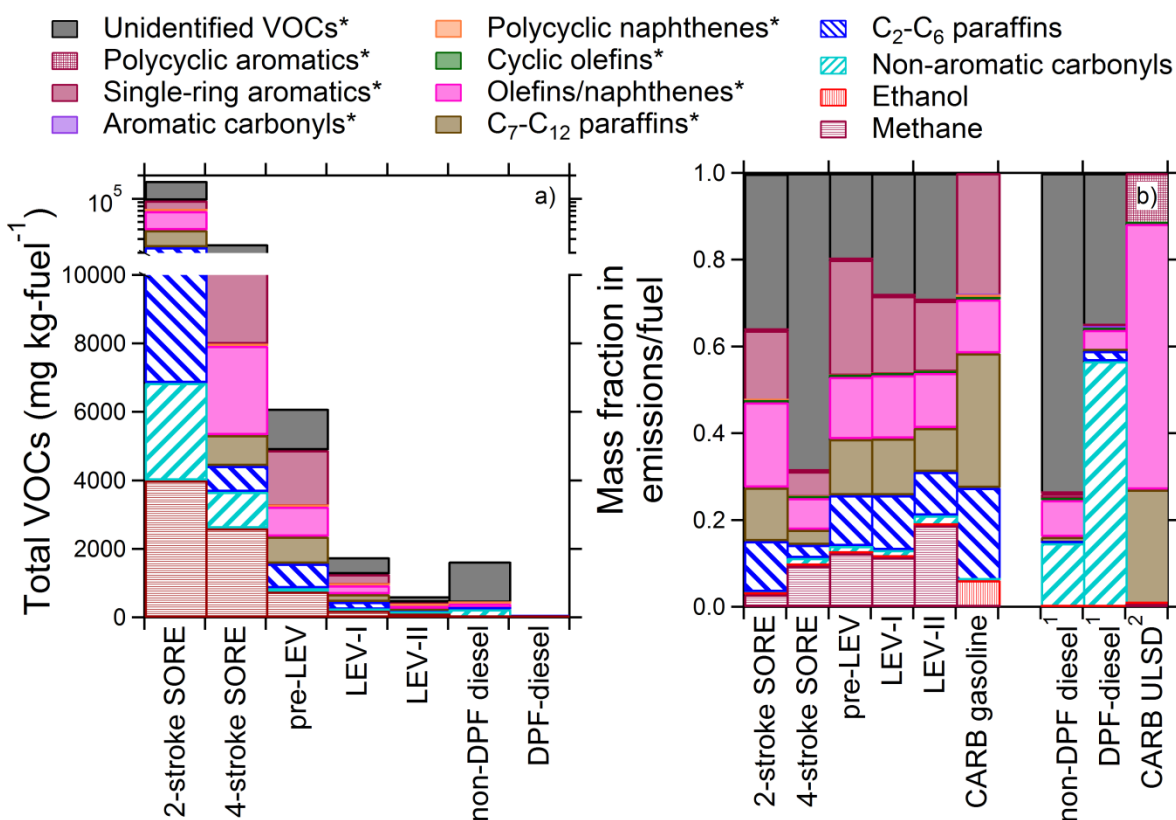


Figure ES-4. Median emissions of speciated VOCs measured from all source categories. **a)** Absolute basis. **b)** Relative basis. Panel (b) also plots data for unburned fuel. Different protocols were used to speciate the gasoline and diesel vehicle exhaust (see text); further, LDGV/MDDVs were tested using vehicle cold start while HDDVs and SOREs followed hot-start procedures. Classes of compounds marked with an asterisk are considered to be SOA precursors. Footnotes: ¹Diesel exhaust speciation protocol different than gasoline. ²Diesel fuel analysis extends to $\sim\text{C}_{30}$

Gas-Particle Partitioning of Primary Organic Aerosol: An important objective of this project was to investigate the gas-particle partitioning of the POA emissions. Mobile sources emit a highly complex mixture of organic compounds, from methane to molecules with more than thirty carbon atoms. These emissions inherently span a wide range in volatility, and POA is the fraction of these emissions that partition into the particle phase in the atmosphere. Recent source testing has suggested that a large fraction of these emissions is semivolatile at atmospheric temperature. The specific technical objectives included: determining whether a large fraction of these emissions is semivolatile at atmospheric conditions, evaluating whether absorption partitioning theory can be used to model the measured changes in gas-particle partitioning, and determining the volatility distribution of the emissions that can be used in

inventories and chemical transport models to quantitatively predict the gas-particle partitioning of the emissions.

Four different methods were used to characterize the gas-particle partitioning of the POA emissions: 1) filter artifact corrections; 2) evaporation induced by dilution of the exhaust from the constant volume sampler into a smog chamber; 3) evaporation induced by heating in a thermodenuder; and 4) volatility distributions derived from gas chromatography analysis. This combination of techniques allowed partitioning measurements to be made across a wide range of atmospherically relevant conditions – temperatures of 25°C to 100°C and organic aerosol concentrations of < 1 to $600 \mu\text{g m}^{-3}$.

The gas-particle partitioning of LDGV POA emissions varied continuously over the entire range of experimental conditions; therefore, none of the POA should be considered non-volatile. For example, isothermal dilution of the emissions between the constant volume sampler and the smog chamber reduced the POA emission factors by about two-thirds. There was additional POA evaporation when the dilute aerosol from the smog chamber was heated in a thermodenuder. By 100°C essentially all of the POA had evaporated. The measured changes in gas-particle partitioning followed absorptive partitioning theory.

Although the magnitude of the LDGV POA emissions varied by more than two orders of magnitude across the entire test fleet, the gas-particle partitioning of these emissions can be described using absorptive partitioning theory and a single volatility distribution. This greatly simplifies accounting for gas-particle partitioning of POA emissions from LDGVs in inventories and models. The recommended volatility distribution for gasoline vehicle POA emissions is listed in Table ES-1. This distribution was derived from results from thermal-desorption gas-chromatography mass-spectrometry analysis of quartz filter samples. It was tested using the measured changes in gas-particle partitioning driven by changes in dilution and temperature. The distribution in Table ES-1, in conjunction with the ΔH_{vap} parameterization of Ranjan, et al. (Aerosol Science & Technology, 46(1), 13-21, 2012), reproduced the measured effects of perturbations to both concentration and temperature on the gas-particle partitioning for the entire test fleet across a wide range of atmospherically relevant conditions. It also distributes the organic material collected on quartz filters into the volatility basis set. Therefore, the distribution

in Table ES-1 can be directly applied to the large archive of quartz filter data for gasoline vehicles to develop emission inventories for chemical transport models, such as the Community Multi-Scale Air Quality model (CMAQ) and the Comprehensive Air Quality Model with Extensions (CAMx), which have implemented the volatility basis set.

For most of the LDGVs tested by this project, the low levels of dilution used in the constant volume sampler created particle concentrations that were a factor of 10 or more higher than typical ambient levels. This resulted in large (factor of 2 or more), systematic partitioning biases in the POA emissions factors compared to more dilute atmospheric conditions. These biases were not an artifact of the test fleet or how the experiments were conducted. The test fleet was comprised of vehicles recruited from the in-use California fleet; the vast majority of these vehicles have very low PM emissions (less than the LEV2 certification standard). The CVS was run following standard Code of Federal Register (CFR) procedures (dilution ratios of ~10-30 at $T = 47 \pm 5$ °C). The data suggest that significant partitioning biases may exist in essentially all gasoline vehicle POA emissions factors currently used in inventories and models, unless they were collected at atmospherically-relevant particle concentrations. The volatility distribution listed in Table ES-1 can be used to correct for these partitioning biases.

Table ES-1. Volatility distributions for gasoline and diesel vehicle POA collected on a quartz filter.

$\log C_i^*$ @ 298K	Gasoline vehicle ¹	Diesel vehicle ¹
-2	0.14 (0.08-0.18)	0.00 (0.00 – 0.01)
-1	0.13 (0.08-0.16)	0.03 (0.02-0.10)
0	0.15 (0.10-0.21)	0.25 (0.12-0.29)
1	0.26 (0.18-0.32)	0.37 (0.30-0.38)
2	0.15 (0.10-0.19)	0.23 (0.17-0.26)
3	0.03 (0.02-0.08)	0.06 (0.04-0.08)
4	0.02 (0.01-0.04)	0.03 (0.02-0.05)
5	0.01 (0.00-0.01)	0.01 (0.01-0.04)
6	0.11 (0.02-0.20)	0.01 (0.00-0.04)

¹ mass fraction of organics collected on a bare-quartz filter. Values indicate median (interquartile range)

Multiple independent approaches indicate that about 80% of the POA emissions from non-DPF-equipped diesel vehicles collected on a quartz filter from a CVS are semi-volatile. For non-DPF-equipped (higher emitting) vehicles, the low levels of dilution used in the CVS created POA concentrations that were much higher than typical ambient concentrations (organic aerosol concentration greater than $100 \mu\text{g m}^{-3}$ in the CVS versus $1\text{-}10 \mu\text{g m}^{-3}$ in the atmosphere). Diluting the exhaust from the CVS to more atmospherically relevant conditions inside a smog chamber caused one-half to two-thirds of the diesel POA to evaporate. Therefore, models and inventories based on emission factors measured in CVS likely over-estimate the contribution of non-DPF-equipped vehicles to ambient POA concentrations. Even at lower, more atmospherically relevant concentrations, a significant fraction of the diesel POA emissions are semivolatile. For example, almost half of the diesel POA at $5 \mu\text{g m}^{-3}$ evaporated when heated in a thermodenuder. Therefore, this dataset provides evidence to the contrary of the widespread assumption that diesel POA emissions are non-volatile at either source testing or atmospheric conditions.

Filter sampling artifacts (adsorbed vapors) depended on the gas-particle partitioning. The relative contribution of artifacts increased for lower emitting vehicles. For very low emitting DPF-equipped vehicles, essentially all of the POA emissions measured on a quartz filter collected from the CVS appear to be adsorbed vapors (sampling artifact). Therefore, correcting for these artifacts is critical for developing robust particle emissions factors.

Although the magnitude of the POA emissions from the individual diesel vehicles varied by more than an order of magnitude across the entire test fleet, the gas-particle partitioning of these emissions can be described using absorptive partitioning theory and a single volatility distribution. The recommended distribution for diesel vehicle POA is listed in Table ES-1. This distribution is designed to be applied directly to quartz filter data that are the basis for existing emissions inventories and chemical transport models that have implemented the volatility basis set approach.

Although the different techniques provided a reasonably consistent picture of the gas-particle partitioning of diesel POA, some uncertainties remain, especially about the lowest volatility tail of the emissions. Heating low concentration emissions in a thermodenuder suggests that as

much as 20% of the organics collected on a quartz filter from the CVS might be classified as effectively non-volatile. In contrast, the dilution and other data suggest that this fraction might be more like 5%. More research is needed to quantify this part of the distribution. However, these issues must be kept in perspective. Most models and inventories assume that 100% of the organics collected on a quartz filter from the CVS are non-volatile. Non-volatile implies no dependence in POA emissions with organic aerosol concentration or temperature, which is inconsistent with essentially the entire dataset except for thermodenuder measurements made at high temperatures and low concentrations.

Secondary Organic Aerosol Formation: Dilute emissions from a subset of the vehicles were transferred from the CVS into a 7 m³ Teflon® smog chamber where they were photochemically aged. The major goals of these experiments were to quantify the fraction of the gas-phase organic emissions that form SOA (yield) and to assess the relative importance of primary PM emissions versus SOA formation. The data collected during these experiments are being used to test and improve SOA modules used in chemical transport models.

Smog chamber experiments were performed with emissions from 15 LDGV, all five diesel vehicles, and two SORE. The experiments were designed to investigate relatively fresh SOA similar to what might be formed in urban environments (modest OH exposures, relatively high NO_x, and moderate organic aerosol concentrations). However, it is impossible to reproduce exactly all atmospheric conditions inside a smog chamber. Therefore, we focused on maintaining several key parameters at urban-like values (e.g., PM concentrations and VOC/NO_x ratios) which are known to strongly influence SOA formation. In most experiments, we added propene (which does not form SOA) to the chamber to adjust the VOC/NO_x ratio to match a typical urban level of ~ 3:1 ppbC/ppbNO_x. This helped ensure that the important radical branching channels such as the fate of organoperoxy radicals (RO₂) were similar to those in the atmosphere. However, values of other parameters were outside of typical atmospheric ranges. Mixing ratios of individual organic gases were typically less than 1 ppb, but were as high as 20 ppbv for the highest emitting vehicle. NO_x levels were between 0.1 and 2.4 ppmv. In addition, the mix of organics inside the chamber (gasoline exhaust + propene) was different than a typical urban atmosphere. Fortunately, SOA yields are thought to be less sensitive to absolute

concentrations, especially if the organic aerosol levels in the chamber are atmospherically relevant. To the extent that the product distribution of the organic oxidation reactions differs from the atmosphere, these differences will influence SOA formation.

Time series of gas and particle concentrations measured during a typical experiment are shown in Figure ES-5. There are three distinct periods in each experiment. First, emissions were added to the chamber causing concentrations of VOCs and NO_x to increase. The second period began when the engine was shut off at time ~ -1 hours. During this period the primary emissions were characterized and nitrous acid (HONO) and propene were added to the chamber. HONO was added to the chamber at approximately time = -0.9 hours to act as a hydroxyl radical source. The addition of HONO increased the NO₂ concentration. The third period began when the UV lights were turned on (time = 0 hours). During the three hours of UV irradiation, primary hydrocarbons were oxidized. There was also rapid and substantial production of SOA, with the suspended organic aerosol concentration increasing from 1 to 17 µg/m³ after the first half an hour of UV exposure. After three hours of photo-oxidation the wall-loss corrected organic aerosol concentrations had increased by roughly a factor of 20 from ~1 µg/m³ of POA to ~22 µg/m³ of mainly SOA.

In essentially every experiment with a gasoline-powered source (LDGV and SORE), three hours of photo-oxidation of dilute tailpipe emissions produced large amounts of SOA inside the smog chamber on both an absolute mass basis and in comparison to the POA emissions. For example, during LDGV experiments, the mass of SOA produced in the smog chamber after three hours of photo-chemistry was three to five times greater than the primary PM mass as measured with filter samples collected from the CVS. For the two-stroke SORE, there was about 14 times more SOA than POA inside the chamber at the end of the experiment. Therefore, SOA will likely be a major component of the contribution of emissions from gasoline-powered sources to ambient PM levels.

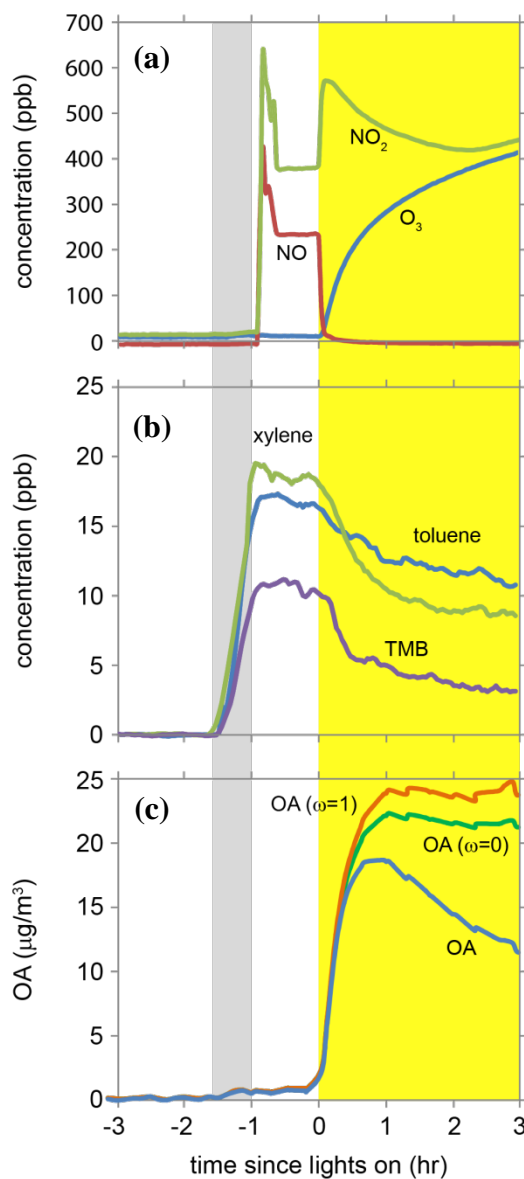


Figure ES-5. Gas-phase and particle-phase evolution during a typical smog chamber experiment (SORE2S-1.1). Between -1.4 hr and -1.0 hr, the chamber was filled with dilute emissions from the backpack blower; between -1.0 hr and 0 hr, the primary PM was characterized; and after 0 hr, the UV lights were on and photo-oxidation generated SOA. Concentrations of NO, NO₂ and O₃ are shown in (a). Shown in (b) are the concentrations of three VOCs which are consumed by OH radicals during the photo-oxidation period. Shown in (c) are uncorrected and corrected (for wall-losses) organic PM concentrations using two different methods ($\omega=0$ and 1); the large increase is due to SOA production.

The data from the LDGV experiments also provides new insight into the effects of vehicle age and drive cycle on SOA formation. The median SOA production (mg/kg-fuel) measured during the cold-start LEV2 experiments was only 38% less than that measured during the median pre-LEV experiment. Some reduction in SOA formation was expected given the large differences in NMOG emissions. However, it was much less than the factor of ten reduction in the NMOG emissions between these two vehicle classes. The median SOA mass formed by three hours of photo-oxidation during a hot-start experiment was only 24% of that formed during the median cold-start experiment (combining all three LEV classes). It is well known that significant emissions occur during cold-start before the catalyst has become active. However, the reduction in NMOG emissions was much larger than SOA formation (hot-start SOA was only a factor of four lower than cold-start). These comparisons underscore the fact that there is not a one-to-one relationship between NMOG emissions and SOA formation, which is not surprising since SOA precursors comprise only a subset of the NMOG emissions.

Although SOA production from diesel vehicles not equipped with a DPF was significant on an absolute basis, after three hours of photo-oxidation the PM levels in the chamber were still dominated by the primary emissions because of the high levels of BC. Therefore, SOA formation from non-DPF-equipped diesel vehicles appears to be relatively less important than the primary PM emissions. SOA production from emissions from the two DPF-equipped vehicles was very low (below the measurement detection limit). However, some SOA formation was measured in experiments conducted with dilute emissions sampled during active DPF regeneration. Further investigation is needed on emissions from passive and active regeneration, but our results support the conclusion that active DPF regeneration contributes relatively little PM over the entire operation cycle (normal driving + regeneration), even when SOA production is included. Therefore, catalyzed DPFs appear to effectively control both primary and secondary PM from diesel vehicles.

The aromatic content of the three different test fuels used in HDDV tests had no effect on the amount of primary PM emissions or SOA production. Therefore, the results suggest that reformulating diesel fuel by altering aromatic content alone is not likely to have a significant impact on either primary or secondary PM. Driving cycle, on the other hand, had a large impact

on SOA production. The large amounts of SOA formed from creep/idle emissions means that efforts to limit idling may be a more effective approach than fuel reformulation to limit the contribution of diesel emissions to ambient PM concentrations.

To investigate the contribution of speciated and unspeciated organics to SOA formation, we calculated an effective yield of the emissions. An effective yield is the fraction of the organic emissions that must be converted to SOA in order to explain the chamber data; it is a standard measure of SOA production in smog chambers. We use the term “effective” yield because LDGV exhaust is comprised of a complex mix of species of which only a subset were quantified by the speciation analysis.

The effective yield analysis indicates that unspeciated NMOG emissions are an important class of precursors in motor vehicle emissions. In fact, the oxidation of unspeciated NMOG emissions appears to contribute the majority of the SOA formation in the hot-start diesel and cold-start LEV1 and LEV2 experiments. The yield analysis also suggests that the mix of organic vapors emitted by newer (LEV2) LDGVs was more efficient (higher yielding) in producing SOA than the emissions from older vehicles.

Motor vehicle exhaust is primarily comprised of saturated compounds, which means that the hydroxyl radical (OH) was the most important oxidant in these experiments. OH levels in the chamber were inferred from the decay of individual gaseous organic compounds. Average OH levels during photo-oxidation were roughly 5×10^6 molecules cm^{-3} , which is representative of summer daytime atmospheric concentrations. Therefore, the smog chamber experiments characterized the effects of a few hours of atmospheric oxidation. Measurements made downwind of urban areas suggest that SOA production continues for about 48 hours at an OH concentration of 3×10^6 molecules cm^{-3} . Therefore, our chamber experiments may underestimate the ultimate SOA formation potential of vehicle emissions.

Separate blank experiments were performed to quantify the potential contribution of contamination. These results are shown in Figure ES-6, which presents the wall-loss-corrected SOA concentrations measured at the end of the 24 cold-start LDGV experiments, three hot-start LDGV experiments, two chamber blank experiments, and nine hot-start experiments performed with catalyzed diesel particulate filter (DPF) equipped heavy duty diesel vehicles. The chamber

blank and hot-start DPF-equipped vehicle data quantify the potential contribution of contamination to the measured SOA formation. A chamber blank followed the same procedures as an actual vehicle test except that the chamber was filled with CVS dilution air only (no vehicle emissions) for the same period of time as the UC. Both primary particle and NMOG emissions from the hot-start DPF-equipped vehicle experiments were extremely low, often below ambient levels; therefore these experiments were essentially equivalent to the blank experiments.

The average wall-loss-corrected SOA mass (assuming no blank correction) for all the cold-start LDGV chamber experiments plotted in Figure ES-6 is $12 \pm 8.4 \mu\text{g m}^{-3}$ which is within the range of typical urban PM concentrations. Therefore the gas-particle partitioning inside the chamber should be representative of the urban atmosphere. The average wall-loss-corrected SOA concentration for the hot-start experiments was much lower, $3.7 \pm 1.4 \mu\text{g m}^{-3}$. Only $1.4 \pm 1.2 \mu\text{g m}^{-3}$ of wall-loss-corrected SOA formed during blank or DPF-equipped vehicle experiments. Therefore the blank corresponded to 12% of the SOA formed in the average cold-start UC experiment. All but two of the LDGV experiments lie above the minimum detection limit (horizontal red line); therefore, the LDGV data are driven by exhaust not contamination.

The SOA measured during blank experiments presumably forms from background organic gases in the CVS dilution air (HEPA-filtered ambient air) and/or organic vapors that desorb from the CVS, transfer line and/or chamber walls. Figure ES-6b plots the estimated fractional contribution of the background organic gases to the chamber based on measurements made at the inlet and exit of the CVS tunnel. During the blank and DPF-equipped experiments, the CVS-dilution air contributed essentially the entire NMOG burden in the chamber. In contrast, during the LDGV experiments the CVS dilution air only contributed a small fraction of the organics to the chamber.

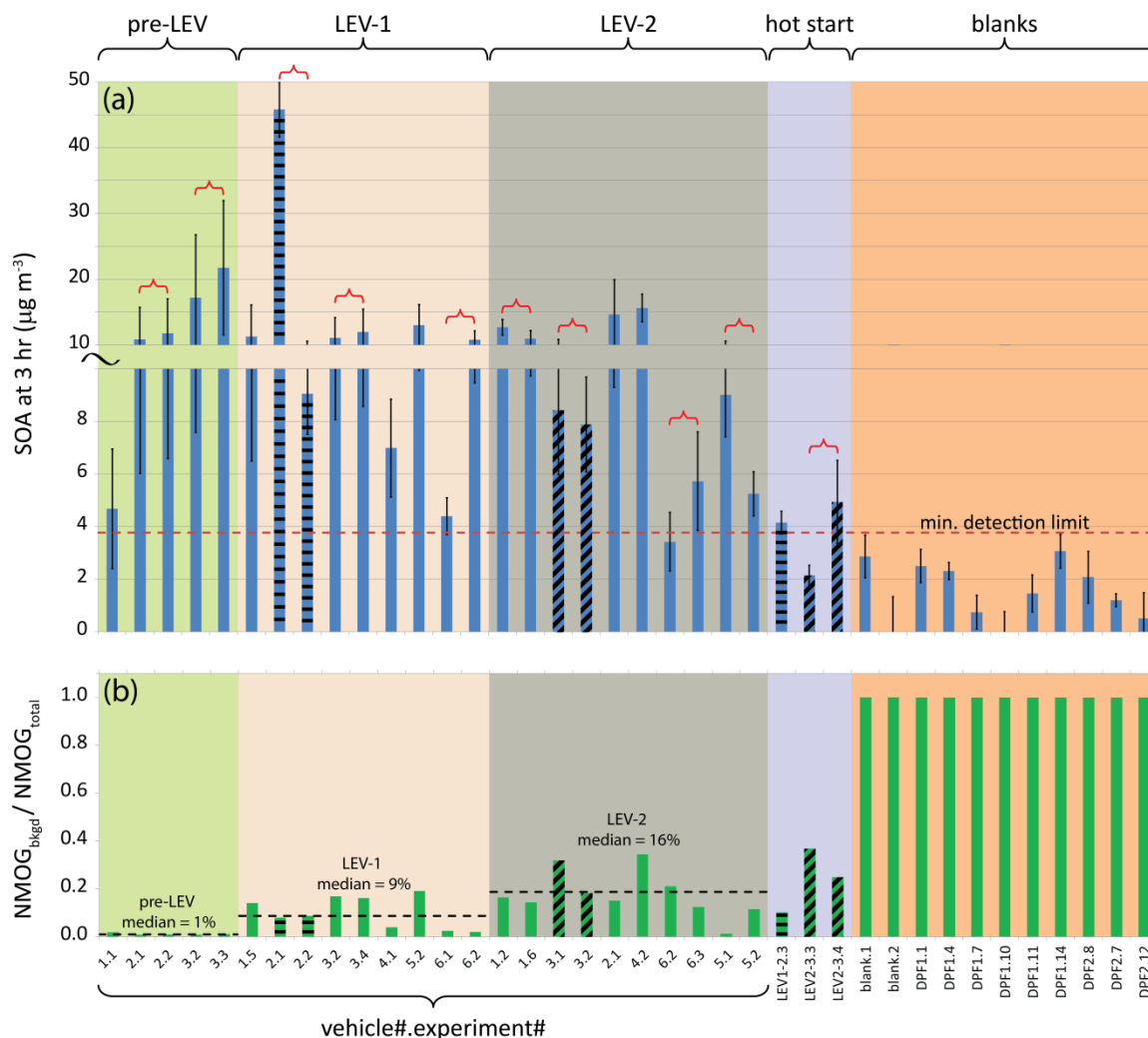


Figure ES-6. (a) Measured wall-loss-corrected SOA concentration inside the smog chamber for LDGV experiments after 3 hours of photo-oxidation and (b) fractional contribution of background NMOG to smog chamber. The red braces in (a) indicate duplicate experiments. Hot-start and normal UC driving cycle experiments with two vehicles (LEV1-2 and LEV2-3) are denoted by the horizontal and diagonal black lines inside of the bars, respectively. The horizontal dashed red line in (a) indicates the minimum detection limit of the experiments. The dashed black lines in (b) indicate the median values of $\text{NMOG}_{\text{bkgd}}/\text{NMOG}_{\text{total}}$ for the three LEV classes.

Synthesis of Particulate Matter Results: The SOA data from the smog chamber experiments and primary PM emissions from the CVS tests are summarized in Figure ES-7. The total height of the bars provides an estimate of the contribution of the emissions to different types of PM after three hours of photo-oxidation in the smog chamber. The primary emissions in Figure ES-7 are medians from the entire vehicle fleet (e.g. all 63 LDGV), while the SOA data are

medians of the chamber experiments, which were only performed on a subset of the LDGV and SORE test fleets. The median values highlight major trends, which are representative of the larger vehicle fleet.

The data presented in Figure ES-7 are presented on a mass of fuel consumed basis to facilitate consistent comparisons between individual emission sources. There are wide differences in fuel consumption between these sources; for example, gasoline consumption in LDGV is much greater than in SORE. This report is focused only on the source-to-source differences.

There are a number of factors that should be considered when evaluating the data in Figure ES-7. First, the primary emissions data shown in Figure ES-7 were measured using quartz filters collected from the CVS. As demonstrated by the gas-particle partitioning measurements performed by this project, the POA emissions factors were biased high relative to more dilute atmospheric conditions due to a combination of partitioning biases and sampling artifacts. Therefore, it is likely that Figure ES-7 overestimates the primary PM levels from an atmospheric perspective. In the atmosphere (and smog chamber), the evaporated POA is oxidized to form SOA. Therefore, the POA and SOA components in Figure ES-7 are not strictly additive. Second, the smog chamber experiments photochemically aged the diluted exhaust for only three hours at atmospherically relevant hydroxyl radical concentrations while field studies have shown that SOA production downwind of urban areas may persist for 48 hours. Therefore, the smog chamber data may underestimate the ultimate production of SOA from dilute exhaust in the atmosphere.

For the sources tested during this project (LDGVs, on-road diesel vehicles and SOREs), 2-stroke gasoline SOREs contributed the most PM in the smog chamber on a mass of fuel basis. The 2-stroke gasoline SOREs had both high primary PM emissions (mainly POA) as well as the most SOA formation. Accounting for both primary PM and SOA, Figure ES-7 indicates that 2-stroke SOREs contribute about 15 times more PM (per mass of fuel consumed) than modern gasoline vehicles (LEV I and LEV II) and about 6 times more than light-duty gasoline vehicles manufactured more than twenty years ago (pre-LEV). The net contribution of 4-stroke SOREs was about a factor of two less than 2-stroke SOREs but still much higher (by at least a factor 2)

than older (pre-LEV) on-road vehicles. Thus, as regulations for on-road gasoline vehicles have reduced their contribution to ambient PM over the last several decades, the role of SOREs has become increasingly important.

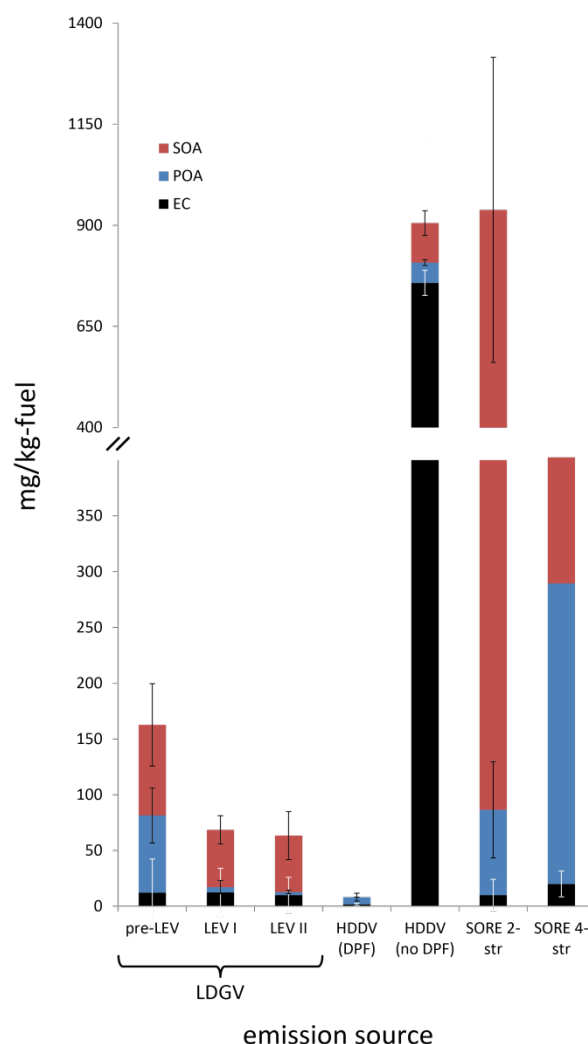


Figure ES-7. Median EC and POA emissions and median SOA production from gasoline small off-road engines (SOREs), light-duty gasoline vehicles (LDGVs) and heavy-duty diesel vehicles (HDDVs). LDGV data were obtained during cold-start UC driving cycle experiments with a single CA summertime gasoline. There are three types of LDGV: pre-LEV vehicles were manufactured before 1995; LEV I vehicles were manufactured between 1995 and 2003; and LEV II vehicles were manufactured after 2003. HDDV data were obtained during UDDS driving cycle experiments with 3 different types of ULSD fuel. The HDDVs were either equipped with a diesel particulate filter (DPF) or no exhaust aftertreatment (no DPF). Error bars represent $\pm 1\sigma$. The absence of error bars for several of the SORE measurements is due to limited data for these sources.

Uncontrolled (no diesel particulate filter) diesels are the only source class tested during this project that contributed a comparable amount of PM as the SOREs. Uncontrolled diesels emitted high levels of primary PM (mainly EC), while SOA was relatively more important for the gasoline-powered SOREs, especially the 2-stroke SOREs. The substantial SOA production from dilute gasoline SORE exhaust is not surprising in light of their very high NMOG emissions.

Newer (LEV1 and LEV2) LDGVs produced less SOA than older (pre-LEV) vehicles (per mass of fuel burned), but the differences were much smaller than the order of magnitude reduction in NMOG emissions. Therefore, for LDGV, the trends in SOA production appear to be more similar to the primary PM emissions than the NMOG emissions. This highlights the complex, nonlinear relationship between NMOG emissions and SOA formation, which is not surprising given that only a subset of the NMOG emissions are SOA precursors. Catalysts are optimized to reduce emissions of regulated pollutants (NO_x , NMOG, and CO), not SOA precursors. They are typically developed using surrogate emissions comprised of small hydrocarbons, such as propene and benzene, many of which do not produce SOA in the atmosphere. Control experiments demonstrated that the SOA production observed during the chamber experiments was not an experimental artifact. Therefore, the data suggest that additional efforts may be needed to optimize catalysts to control SOA precursor emissions to further reduce the contribution of LDGV to ambient PM.

Figure ES-7 indicates that hot-start emissions from vehicles equipped with DPFs had the lowest contribution to PM of any of the sources tested during this project. They had both very low primary PM emissions as well as negligible SOA formation. Therefore, catalyzed diesel particulate filters appear to be a very effective emissions control technology.

List of Publications

The results summarized in this report are described in detail in seven peer-reviewed publications:

1. “Gas- and particle-phase primary emissions from in-use, on-road gasoline and diesel vehicles” (May, A. A.; Nguyen, N. T.; Presto, A. A.; Gordon, T. D.; Lipsky, E. M.; Karve, M.; Gutierrez, A.; Robertson, W. H.; Zhang, M.; Brandow, C.; Chang, O.; Chen, S.; Cicero-Fernandez, P.; Dinkins, L.; Fuentes, M.; Huang, S.-M.; Ling, R.; Long, J.; Maddox, C.; Massetti, J.; McCauley, E.; Miguel, A.; Na, K.; Ong, R.; Pang, Y.; Rieger, P.; Sax, T.; Truong, T.; Vo, T.; Chattopadhyay, S.; Maldonado, H.; Maricq, M. M.; Robinson, A. L.) *Atmospheric Environment*, 88, 247-260, 2014.
<http://www.sciencedirect.com/science/article/pii/S1352231014000715>
2. “Secondary Organic Aerosol Formation Exceeds Primary Particulate Matter Emissions for Light-Duty Gasoline Vehicles” (T.D. Gordon, N.T. Nguyen, A.A. Presto, N.M. Donahue, A. Gutierrez, M. Zhang, C. Maddox, P. Rieger, S. Chattopadhyay, H. Maldonado, M. M. Maricq, A. L. Robinson), *Atmospheric Chemistry and Physics*, 14, 4661–4678, 2014.
<http://www.atmos-chem-phys.net/14/4661/2014/acp-14-4661-2014.html>
3. “Secondary Organic Aerosol Production from Diesel Vehicle Exhaust: Impact of Aftertreatment, Fuel Chemistry and Driving Cycle” (T.D. Gordon, A.A. Presto, N.T. Nguyen, W.H. Robertson, K. Na, K. N. Sahay, M. Zhang, C. Maddox, P. Rieger, S. Chattopadhyay, H. Maldonado, M.M. Maricq, A. L. Robinson), *Atmospheric Chemistry and Physics*, 14, 4643–4659, 2014. <http://www.atmos-chem-phys.net/14/4643/2014/acp-14-4643-2014.html>
4. “Primary Gas- and Particle-Phase Emissions and Secondary Organic Aerosol Production from Gasoline and Diesel Off-Road Engines” (T.D. Gordon, D.S. Tkacik, A.A. Presto, M. Zhang, S.H. Jathar, N.T. Nguyen, J. Massetti, T. Truong, P. Cicero-Fernandez, C. Maddox, P. Rieger, S. Chattopadhyay, H. Maldonado, M.M. Maricq, A.L. Robinson), *Environmental Science & Technology*, 47 (24), 14137–14146, 2013.
<http://pubs.acs.org/doi/abs/10.1021/es403556e>
5. “Primary to secondary organic aerosol: evolution of organic emissions from mobile combustion sources” (A. A. Presto, T. D. Gordon, and A. L. Robinson) *Atmospheric Chemistry and Physics*, 14, 5015-5036, 2014. <http://www.atmos-chem-phys.net/14/5015/2014/acp-14-5015-2014.html>
6. “Gas-particle partitioning of primary organic aerosol emissions: (2) diesel vehicles” (A. A. May, A. A. Presto, C. J. Hennigan, N. T. Nguyen, T. D. Gordon, A. L. Robinson) *Environmental Science & Technology*, 47 (15), 8288–8296, 2013.
<http://pubs.acs.org/doi/abs/10.1021/es400782j>
7. “Gas-particle partitioning of primary organic aerosol emissions: (1) gasoline vehicle exhaust” (A. A. May, A. A. Presto, C. J. Hennigan, N. T. Nguyen, T. D. Gordon, A. L. Robinson) *Atmospheric Environment*, 77, 128-139, 2013.
<http://www.sciencedirect.com/science/article/pii/S1352231013003245>